



A GENERALIZED VERSION OF DUPORCQ'S EQUATION

Veturia CHIROIU^{*}, Cornel BRISAN^{**}, Ligia MUNTEANU^{*}

^{*} Institute of Solid Mechanics, Romanian Academy, Bucharest

^{**} Technical University of Cluj-Napoca, Cluj-Napoca

Corresponding author: Ligia Munteanu, E-mail: ligia_munteanu@hotmail.com

Abstract Ernest Duporcq proposed in 1898 a theorem having as object the rigid-body motions with spherical trajectories. The theorem says that if five points situated on a moving plane P move on five fixed spheres with centers on a fixed plane P' , then there exists on P a sixth point which also describes such a sphere. More clearly, given five points in P and five points in P' , then there exists an additional pair of points which also describes a sphere. The original scientific contribution of this paper consists in a generalized version of this theorem: *Given five points on a moving plane P and five points in a fixed plane P' , that are moving on the super-ellipsoidal trajectories*

$$F(x) = \left[\left(\frac{x}{r_1} \right)^{2/\varepsilon_1} + \left(\frac{y}{r_2} \right)^{2/\varepsilon_1} \right]^{\varepsilon_1/\varepsilon_2} + \left(\frac{z}{r_3} \right)^{2/\varepsilon_2} - 1$$

then there exists an additional pair of points which describe such a super-ellipsoidal trajectory. According to this version, the trajectories of a moving body defined by six distance or/and angular constraints between six pairs of points, lines and/or planes, are identified by intersections of two super-ellipsoids. These motions are of interest for simulation, control and performance design of Stewart-Gough platforms in order to prevent their destruction due to the chaotic behavior. The dynamics of such platforms can be extremely complicated due to the riddling bifurcation and the appearance of the hyperchaotic attractors.

Key words: Duporcq's theorem, super-ellipsoidal trajectories, Stewart-Gough platforms, riddling bifurcation, hyperchaotic attractors.

1. INTRODUCTION

Duporcq theorem (1898) says that if five points situated of a moving plane P move on five fixed spheres with centers on a fixed plane P' , then there exists a point on P which describes a sphere [1]. As an interesting detail, the French Academy of Science has launched in 1904 the *Prix Vaillant* competition with the theme of searching all displacements of a rigid body for which distinct points move on a spherical trajectory [2]. Borel [3] and Bricard [4] received the prize and the *Borel-Bricard problem* becomes important in recent years due to the Stewart-Gough platforms applications [5-13].

The Navwratil version of Duporcq's theorem (2014) is [14]: "If five pairs of attachment points $(b_i, a_i) \neq (b_j, a_j)$, $j \neq i$, $i, j \in \{1, 2, \dots, 5\}$ of a planar manipulator are given, then there exists a sixth

point pair $(b_6, a_6) \neq (b_k, a_k)$, $k = 1, 2, \dots, 5$, such that the resulting planar architecturally singular manipulator has the same solution for the direct kinematics as the first one, where the pair (b_l, a_l) , $l = 1, 2, \dots, 6$, verifies the conditions: a) sphere condition, if b_l and a_l are finite; b) Darboux condition, if b_l is finite and a_l is an ideal point; c) Mannheim condition, if b_l is an ideal point and a_l is finite; d) angle condition, if b_l and a_l are ideal points”.

A sphere of center A which passes through B is defined as a set of points having the same distance from A to B . The sphere condition is verified if B_l and A_l are finite. The sphere condition transforms in the *Darboux condition* when the center A tends to ∞ and B is finite. In this case, the point B is located in a fixed plane orthogonal to the direction of the ideal point A . The Darboux condition is verified if B_l is finite and A_l is an ideal point. By changing the role of the fixed and moving platforms, the sphere condition transforms in the *Mannheim condition*. This condition is verified if B_l is an ideal point and A_l is finite. This means that a plane of the moving orthogonal system to the direction of the ideal point B slides through A . The Mannheim motion is the inverse of the Darboux motion. If A is an ideal point, the finite point B can be reflected on all finite planes through A . The resulting points form a plane through B orthogonal to A , and the Darboux condition is verified. The inverse Darboux conditions yields to the Mannheim condition. The ideal points have the property that each point encloses the same angle ϕ with the ideal point A , and the point B can be reflected on all finite planes through A . This condition is known as *the angle condition*.

The new version of the Duporcq's theorem considers that the spatial motions of a moving body have the super-ellipsoidal trajectories in the 3D Euclidean space. In this way, a large number of motions of a Stewart-Gough platform is identified, including the known ones, by intersections of two super-ellipsoids.

The Stewart-Gough platforms are mechanisms composed of two rigid objects, a base and a platform, connected by six legs through spherical joints. A class of these platforms is architecturally singular being characterized by motions determined only by its geometry [15-24].

This article is focused on the self-motions of a class of the architectural singular Stewart-Gough platforms, i.e. the Segre-dependent Stewart-Gough platforms in which each leg has a linear condition under the Segre embedding related to the Euclidean group $SE(3)$ consisting of rotations and translations in R^3 [25]. The dynamics of these platforms can include the riddling bifurcation, i.e. the bifurcation in which one of the unstable trajectory embedded in a higher-dimensional chaotic attractor becomes unstable transversely to the attractor [26-28]. When a trajectory leaves an attractor, it can be attracted by another attractor and therefore, the riddling phenomenon appears, and then automatically the generation of the hyperchaotic attractors [29-35].

The paper is organized as follows: Section 2 is devoted to new version of the Duporcq's theorem. In Section 3, the trajectories of distinct points of the body are determined by intersecting of two super-ellipsoids. The road to chaos of a class of the architectural singular Stewart-Gough platforms, is presented in Section 4. The conclusions are drawn in Section 5.

2. A NEW VERSION OF THE DUPORCQ'S THEOREM

Let us to present a generalized version of the Duporcq's theorem:

If five pairs of attachment points $(b_i, a_i) \neq (b_j, a_j)$, $j \neq i$, $i, j = 1, 2, \dots, 5$ of a planar manipulator are moving of super-ellipsoidal trajectories, $a_i \in F_1 \geq 0$ and $b_i \in F_2 \geq 0$, $i = 1, 2, \dots, 5$, where F is defined as

$$F(x) = \left[\left(\frac{x}{r_1} \right)^{2/\varepsilon_1} + \left(\frac{y}{r_2} \right)^{2/\varepsilon_1} \right]^{\varepsilon_1/\varepsilon_2} + \left(\frac{z}{r_3} \right)^{2/\varepsilon_2} - 1, \quad (1)$$

then there exists a sixth point pair $(b_6, a_6) \neq (b_k, a_k)$, $k = 1, 2, \dots, 5$, in a way that the resulting planar architecturally singular platform has the same solution for the direct kinematics as the given one, and the sixth point pair (b_6, a_6) fulfills the same condition of super-ellipsoidal. This condition refers to that all attachments points move on two super-ellipsoids.

The proof of this theorem is easily done by intersecting two super-ellipsoids $F_1 \geq 0$ and $F_2 \geq 0$. By these intersections, the trajectories of distinct points of the body are obtained. The constants r_i , $i = 1, 2, 3$, and ε_i , $i = 1, 2$, are determined from the condition that displacements of both platforms move on two super-ellipsoids. In addition, if five pairs of attachment points $(b_i, a_i) \neq (b_j, a_j)$, $j \neq i$, $i, j \in \{1, 2, \dots, 5\}$ of a planar platform are given, then there exists a sixth point pair $(b_6, a_6) \neq (b_k, a_k)$, $k = 1, 2, \dots, 5$, in a way that the resulting planar architecturally singular manipulator has the same solution for the direct kinematics. Instead, additional conditions of the Darboux, Mannheim or angle are not necessary to be verified because they are immediately met for finite and ideal points.

The $x = (r, \theta, z)$ represents the spatial cylindrical (Eulerian) coordinates, centred in O , and $x_1 = r \cos \theta$, $x_2 = r \sin \theta$, $x_3 = z$. The x_3 -axis corresponds to the z -axis of inertia of the super ellipsoid model. A point x with $F(x) < 0$ is inside the super-ellipsoid and every point x with $F(x) = 0$ lies on its surface. The radius r_i , $i = 1, 2, 3$, gives the size of the super-ellipsoid. The exponents $\varepsilon_1, \varepsilon_2 \in (0, 2)$ correspond to a convex body and $\varepsilon_i \rightarrow 0$ yields a cuboid and $\varepsilon_i \rightarrow 2$ an octahedron. The distance between P and P' belonging to S must be minimized

$$\min \left(\frac{1}{2} (x_1 - x_2)^T (x_1 - x_2) \right), \quad (2)$$

where x_1 and x_2 are the position vectors of the points, respectively.

The task is to determine the unknowns r_i and ε_i , $i = 1, 2$, so that all points of a rigid body move on super-ellipsoidal trajectories. Conform to this statement, the sixth point pair can change with respect to different values for the lengths of the first five legs.

The super-ellipsoid can be written in terms as

$$x(\psi, \theta) = \begin{bmatrix} \text{sgn}(\cos \psi) & r_1 |\cos \psi|^{\varepsilon_1} & |\cos \theta|^{\varepsilon_2} \\ \text{sgn}(\sin \psi) & r_2 |\sin \psi|^{\varepsilon_1} & |\cos \theta|^{\varepsilon_2} \\ \text{sgn}(\sin \theta) & r_3 |\sin \theta|^{\varepsilon_2} & 0 \end{bmatrix}, \quad \psi \in [-\pi, \pi], \quad \theta \in [-\pi/2, \pi/2]. \quad (3)$$

We rewrite (1) under the form

$$-F^2(x) \geq 0. \quad (4)$$

By intersection of two super-ellipsoids $F_1 \geq 0$ and $F_2 \geq 0$, we obtain

$$F_{\text{int}} = (-F_1^2) \wedge (-F_2^2) \geq 0, \quad (5)$$

where \wedge is the intersection operator defined as

$$f_1 \wedge f_2 = f_1 + f_2 - \sqrt{f_1^2 + f_2^2}. \quad (6)$$

Summing up, the super-ellipsoids are topologically equivalent to spheres. The spheres can be

considered as ellipsoids with axes r_1, r_2, r_3 whose curvature in the (x, y, z) direction is distorted by the influence of the exponents ε_1 and ε_2 . The exponents ε_1 and ε_2 possess a great flexibility for obtaining new object with interesting shape.

3. INTERSECTION DETECTION ALGORITHM

The intersection detection algorithm has to find if two points $P_1 \in F_1$ and $P_2 \in F_2$ are in contact. The distance of penetration $d = \|P_2 - P_1\|$ and the contact direction c verify $n_1 = \mu^2 c$ and $n_2 = -\nu^2 c$, $d \times c = 0$ where n_1 and n_2 are the outward surface normal at P_1 and P_2 , and μ, ν are arbitrary real numbers.

A scheme of trajectories is shown in Fig. 1, where the bottom platform consists of six legs located at a_i , $i = 1, 2, \dots, 6$. The corresponding moving platform has the attachments b_i , $i = 1, 2, \dots, 6$. The theorem identifies many manipulators. In contrast to known Stewart-Gough platforms which six constraints in distances between points, the theorem permits to find Stewart-Gough platforms with six distance or/and angular constraints between six pairs of points, lines, and/or planes in the base and platform, respectively.

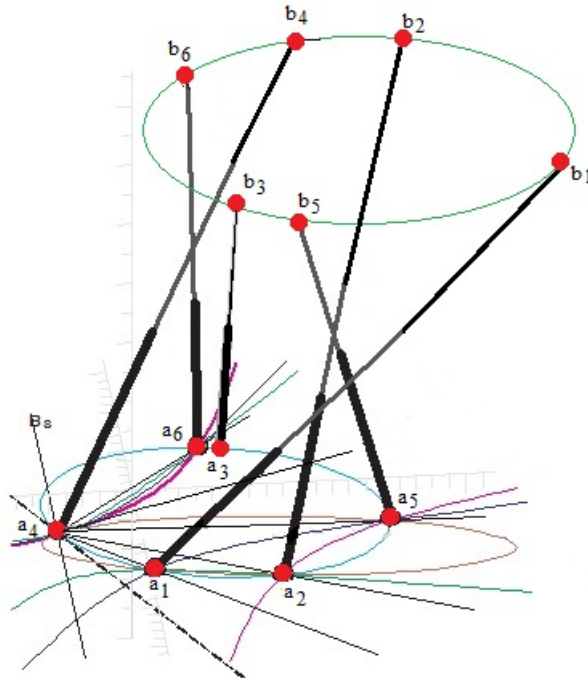


Fig. 1. Scheme of trajectories obtained by the intersections of two super-ellipsoids.

The sets of points, planes, and lines in 3D Euclidean space are subjected to geometric constraints: the distance constraints between point/point, point/line, point/plane, line/line, and the angular constraints between line/line, line/plane, and plane/plane. Therefore, to determine the manipulator position and orientation, six geometric constraints are needed.

The platforms include four types of constraints: (1) three distances and three angular constraints, (2) four distances and two angular constraints and (3) five distances and one angular constraints and (4) six distance constraints. In this context, the literature reports 1120 motions of the first type, 1260 of the second type, 1008 of the third type, and 462 of the last type [14].

The resulting planar architecturally singular Stewart-Gough platforms has the same solution for

the direct kinematics as the given one, where the pair (b_l, a_l) , $l = 1, 2, \dots, 6$, verify the super-ellipsoid condition.

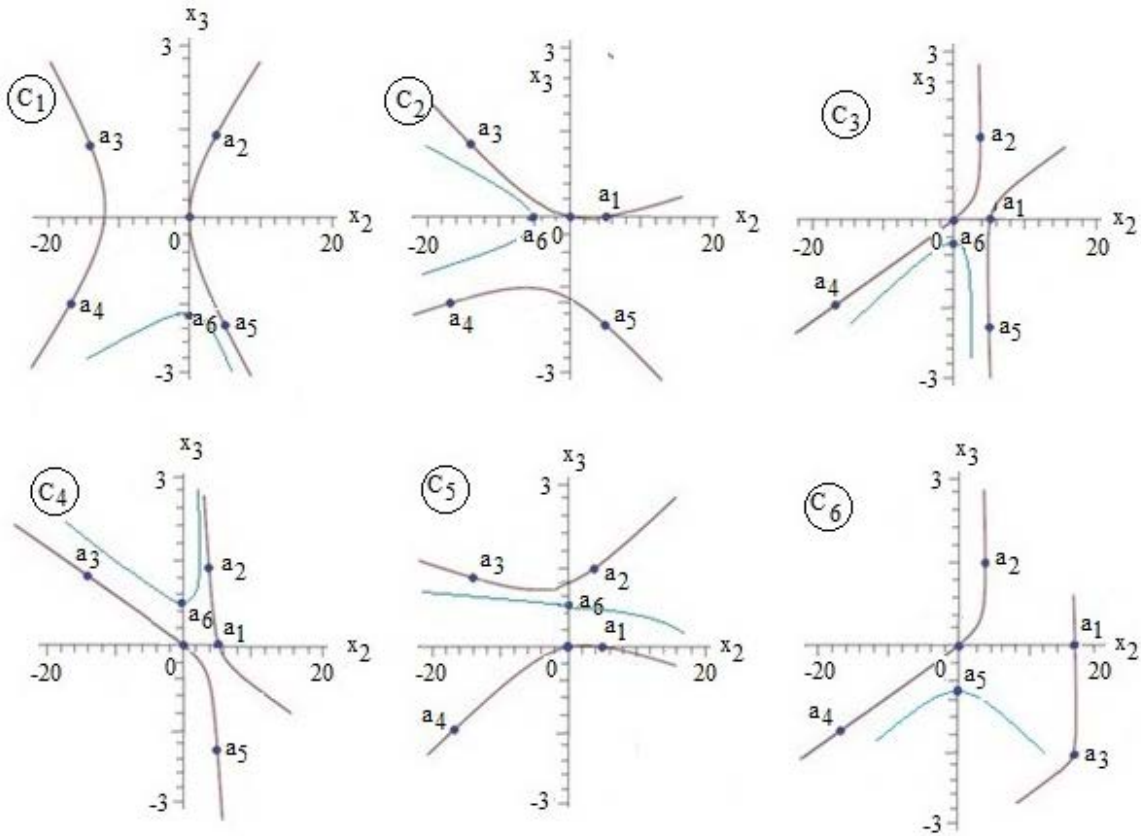
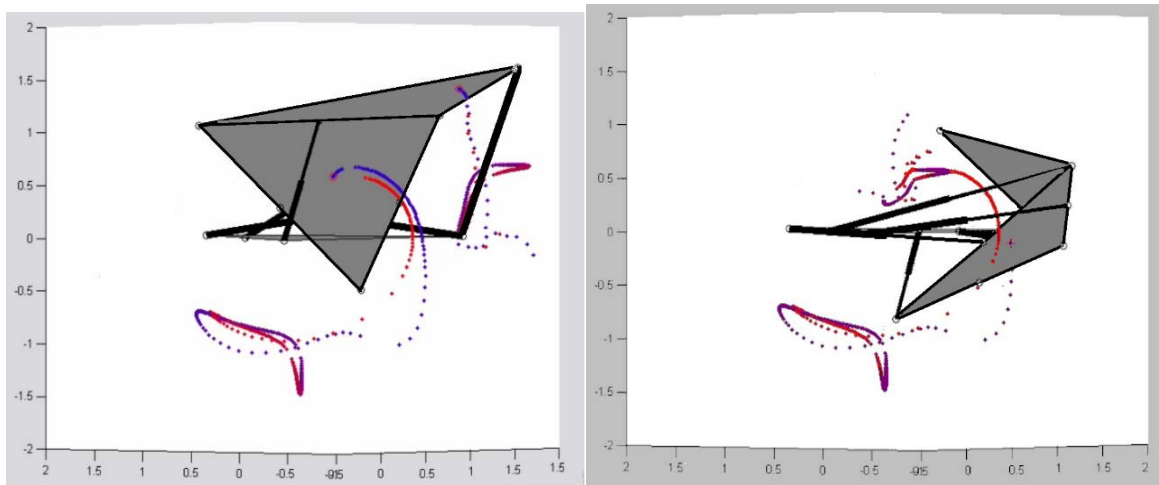


Fig. 2. Sectional curves obtained by intersection of two super-ellipsoids with plane-body component.

The motion is as follows: if P' moves parallelly to P , so that one of its points traces out a fixed line perpendicular to P , and another point is on a fixed super-ellipsoid with center on the same plane, then all the points of the space attached to P' move on super-ellipsoidal curves. Some sketches during the motion of a singular Stewart-Gough platform with plane-body component are displayed in Fig.3.



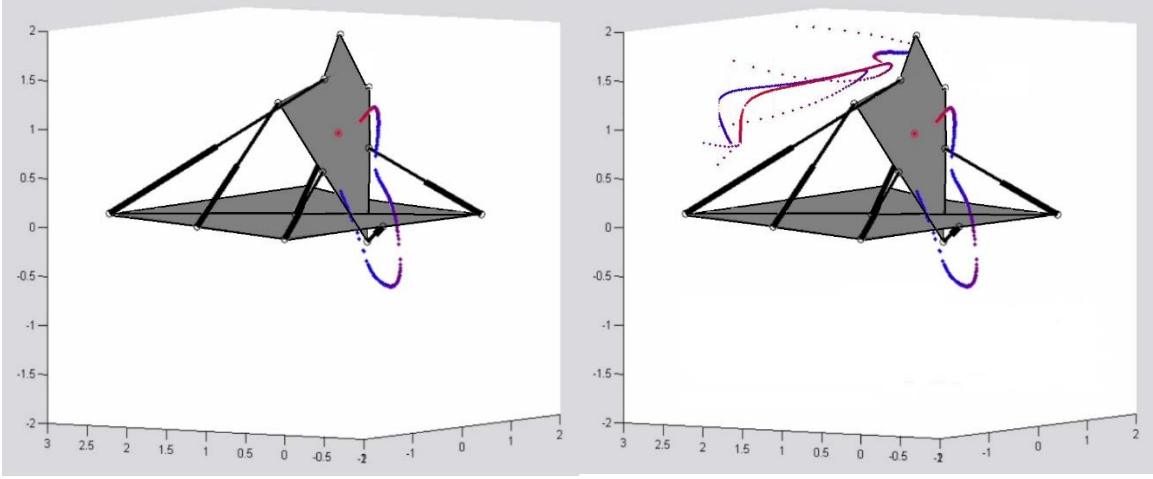


Fig. 3. Sketches of motion of a singular Stewart-Gough platform with plane-body component.

In contrast to the known Stewart-Gough platforms which have only six constraints in distances between points, the theorem permits determining the Stewart-Gough platforms with six distance or/and angular constraints between six pairs of points, lines, and/or planes in the base and platform, respectively.

By intersection of two super-ellipsoids different sectional curves C_i , $i = 1, 2, \dots, 6$, are obtained. Six curves are illustrated in Fig. 2 for $r_1 = r_2 = r_3 / 2$, and $\varepsilon_i = 0.3$, for a plane-body component.

4. ROAD TO CHAOS OF THE SEGRE-DEPENDENT STEWART-GOUGH PLATFORMS

We consider the class Segre-dependent Stewart-Gough platforms of the architectural singular Stewart-Gough platforms, in which each leg has a linear condition under the Segre embedding related to the Euclidean group $SE(3)$ consisting of rotations and translations in R^3 [36]. The distance constraint of each leg corresponds to the intersection of $SE(3)$ with a hyperplane. Consider the case when the platform moves along one of the sectional curves C_i , $i = 1, 2, \dots, 6$, obtained by intersection of two super-ellipsoids, keeping the same relative rotation with respect to base (Fig.4).

Sectional curves are correlated with each other by a reciprocally interaction. This dynamic interaction leads to the chaos behavior if one of the curve, let's say C_0 , is perturbed. To investigate the behavior of the Euclidean distance in the phase space $(C_i, C_{i,\tau})$ between a perturbed curve and another curve C_i , we consider

$$D(\tau) = \sqrt{\sum_{i=1}^6 (x_i^0 - x_i^1)^2 + \sum_{i=1}^6 (x_i'^0 - x_i'^1)^2 \tau^2}, \quad (7)$$

where τ is the time, the superscript 0 indicates the non-perturbed curve and 1 the perturbed one, respectively.

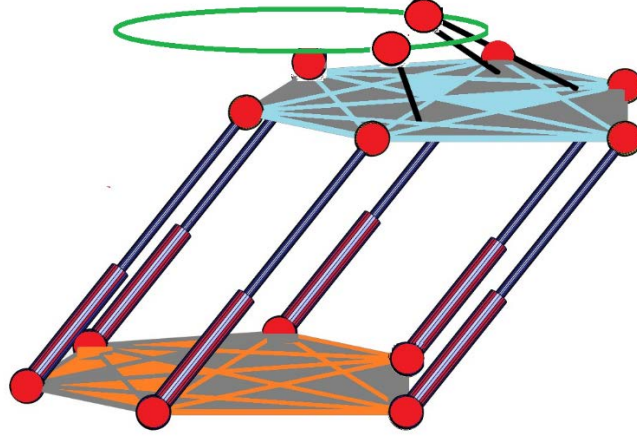


Fig.4. A Stewart-Gough platform with motion along a curve $C \in C_i, i = 1, 2, \dots, 6$.

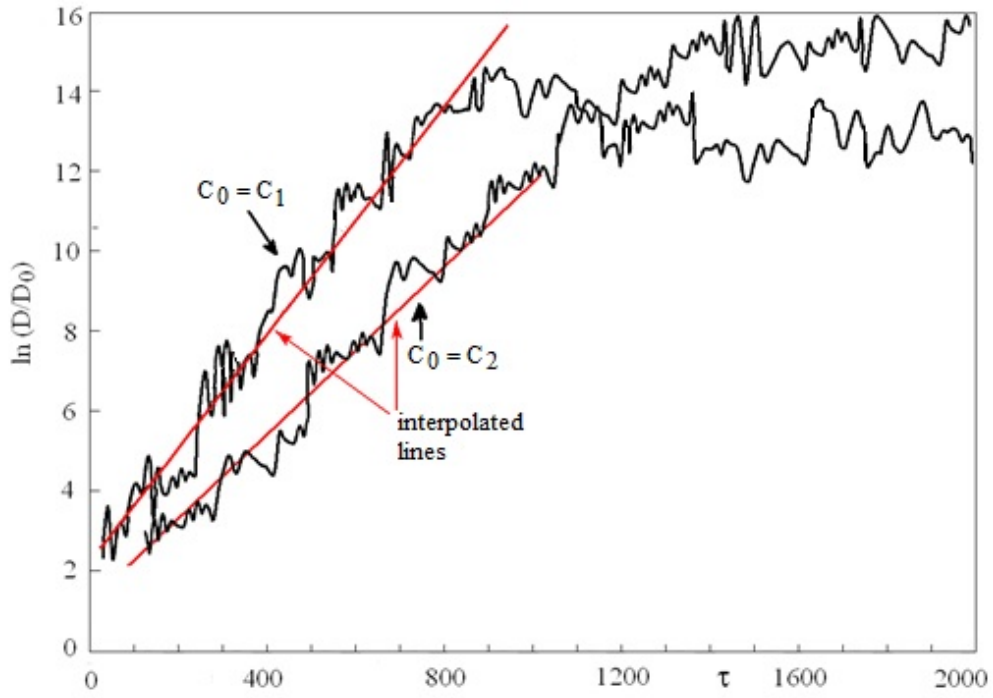


Fig. 5. Time dependence of $\ln(D(\tau)/D_0)$ for $C_0 = C_1$ and $C_0 = C_2$, respectively.

The initial perturbation applied to the curve C_0 is $D_0 = 2 \times 10^{-3}$. $D(\tau)$ is a linear function at short intervals of time, but for long intervals of times, the function shows an exponential increasing. This behavior of $D(\tau)$ is characteristic to the chaotic motion at short intervals of time and can be characterized by the Lyapunov exponent λ

$$\exp(\lambda\tau) = \lim_{d_0 \rightarrow 0} D(\Delta\tau) / D_0. \quad (8)$$

The time variation of $\ln(D(\tau)/D_0)$ for the body is presented in Fig. 5. The red lines are the interpolated lines used to calculate the Lyapunov exponent [36]. The time variation of $\ln(D(\tau)/D_0)$ may define the thresholds between regular and chaotic motions with respect to C_0 .

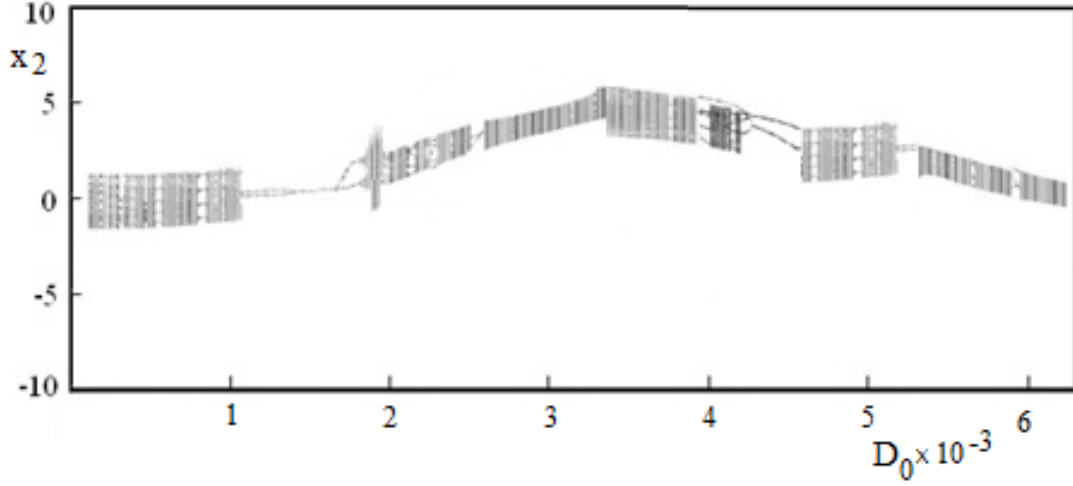


Fig. 6. Bifurcation diagrams of x_2 as a function of D_0 .

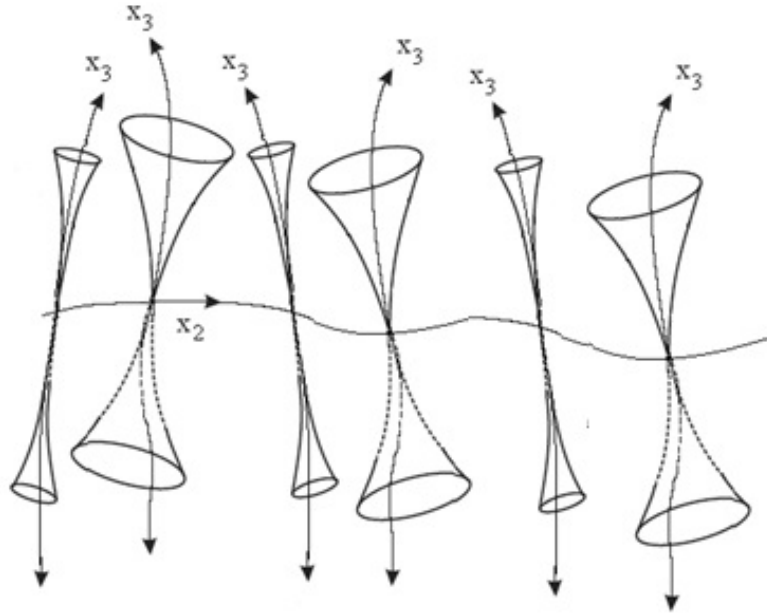


Fig. 7. Riddling bifurcations of the unstable periodic orbits with respect to x_2 and x_3 .

Numerical results shown that the initial perturbation D_0 applied to a curve C_0 affects stability of the periodic orbits. The orbits become unstable in the least two directions in the vicinity of a transition point. Fig. 6 plots the bifurcation diagrams showing the asymptotic values of x_2 versus the initial perturbation D_0 applied to $C_0 = C_1$. The orbits (x_2, x_3) exhibit the riddling bifurcation expressed as tongues anchored at these orbits, as shown in Fig. 7 [39]. The transition between the chaos and hyperchaos is done by an infinite number of tongues that appear simultaneously in the least two directions in the vicinity of a transition point. The bifurcation of an unstable periodic orbit is characteristic for the chaos-hyperchaos transition.

The Poincaré cross-section is determined by normal vector chosen along the curve C_0 . The period of solutions is determined by using the symbolic dynamics of the map in the spirit of [34-36]. Fig. 8a shows the 2D projection of the Poincaré map into the plane (x_2, x_3) of the chaotic attractor with two-bundle, for $C_0 = C_1$ and one positive Lyapunov exponent $\lambda_1 = 0.42$. For $C_0 = C_2$, the Lyapunov exponent is $\lambda_1 = 0.62$ and the 2D projection of the Poincaré map into the plane (x_2, x_3) of the chaotic attractor with two-bundle is shown in Fig. 8b.

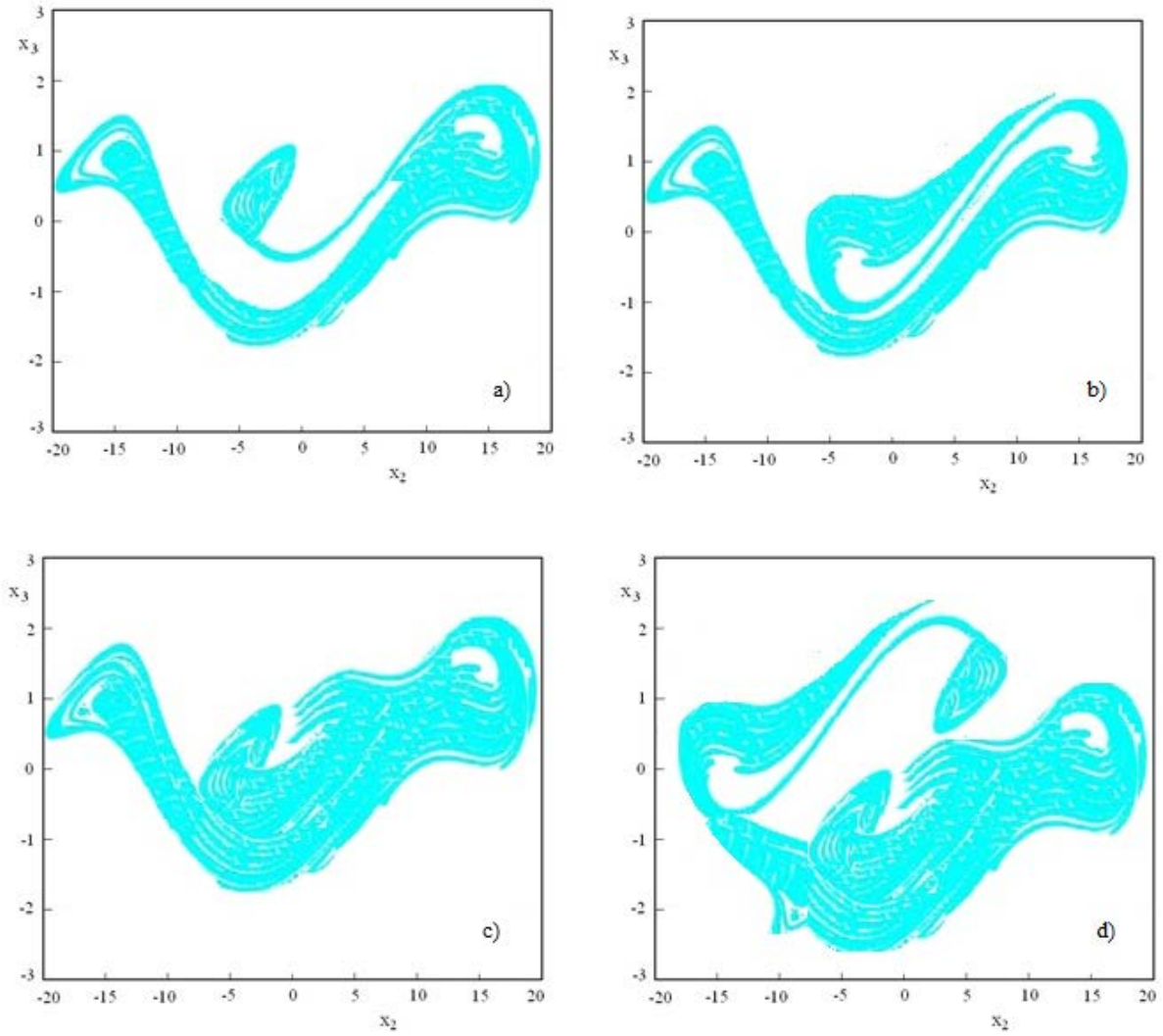


Fig. 8. 2D projection of the Poincaré map into the plane (x_2, x_3) of the attractor a) chaotic for $C_0 = C_1$; b) chaotic for $C_0 = C_2$; c) hyperchaotic for $C_0 = C_1$ and $C_0 = C_2$; and d) hyperchaotic for $C_0 = C_1$, $C_0 = C_2$ and $C_0 = C_3$.

If two curves, let's say $C_0 = C_1$ and $C_0 = C_2$ are perturbed, two Lyapunov exponents $\lambda_1 = 0.41$ and $\lambda_2 = 0.33$ are obtained, and the resulting attractor is a hyperchaotic one, as shown in Fig. 6c. Fig. 8d shows a hyperchaotic attractor when three curves $C_0 = C_1$, $C_0 = C_2$ and $C_0 = C_3$ are perturbed and three Lyapunov exponents $\lambda_1 = 0.75$, $\lambda_2 = 0.63$ and $\lambda_3 = 0.44$ are obtained. The transition to hyperchaos is characterized by an infinite number of unstable periodic orbits which becomes unstable in the least two directions in the vicinity of a transition point. The bifurcation of an unstable periodic orbit is characteristic for the chaos-hyperchaos transition.

The initial basin of attraction is growing after the riddling bifurcations. This means the orbits expand in directions x_2 and x_3 . The enlargement aspect of the attractors shown in Fig. 9 for a) $C_0 = C_1$ and b) $C_0 = C_2$, respectively. The chaotic behavior leads finally to the destruction of the platform, as shown in Fig.10, by the detachment of the legs.

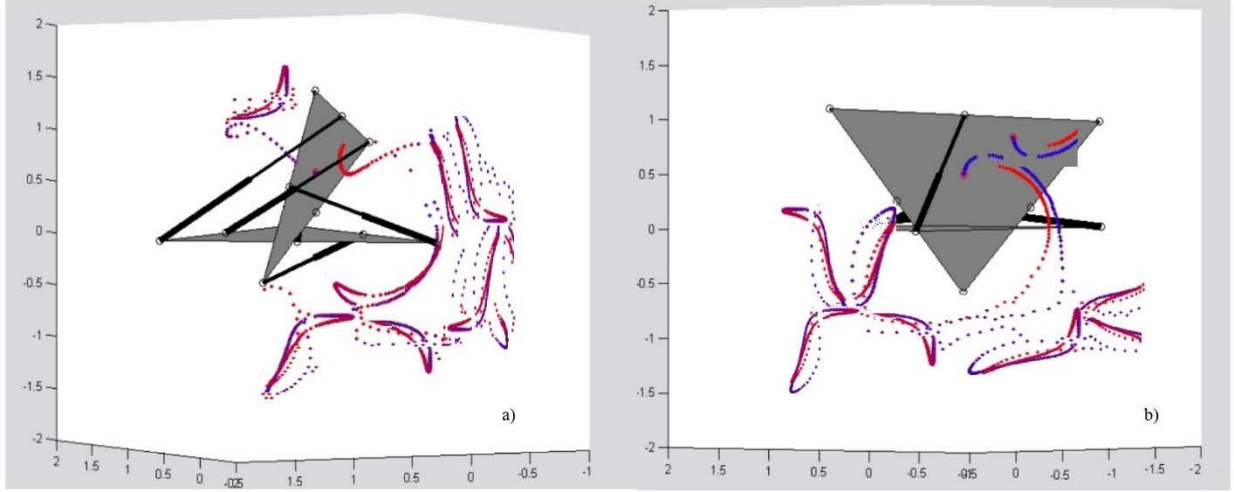


Fig. 9. The growing of the chaotic attractor for a) $C_0 = C_1$ and b) $C_0 = C_2$, respectively.

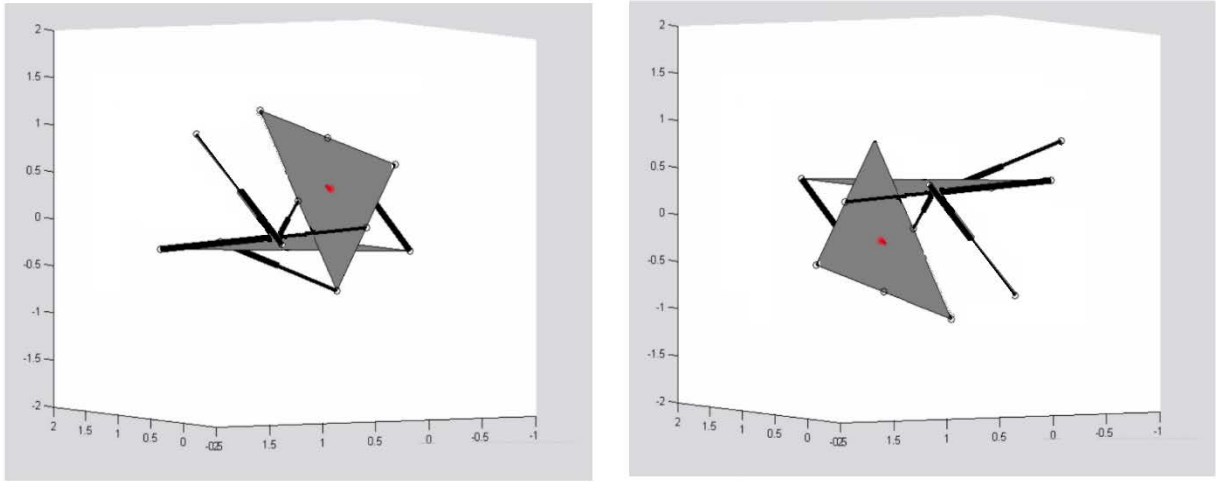


Fig. 10. Types of broking of the platform for a) $C_0 = C_1$ and b) $C_0 = C_2$, respectively.

5. CONCLUSIONS

The numerical simulations of the spatial motions described in this paper have the property that all points of the moving body have super-ellipsoidal trajectories. The key features of such motions result from the new version of the Duporcq's theorem by the intersection of two super-ellipsoids in the 3D Euclidean space. The theorem states that if five pairs of attachment points $(b_i, a_i) \neq (b_j, a_j)$, $j \neq i$, $i, j = 1, 2, \dots, 5$, of a planar manipulator are moving of super-ellipsoidal trajectories, then there exists a sixth point pair $(b_6, a_6) \neq (b_k, a_k)$, $k = 1, 2, \dots, 5$, such that the resulting planar singular platform has the same solution for the direct kinematics as the first one, and the sixth point pair (b_6, a_6) moves on the super-ellipsoid. This theorem identifies a larger number of configurations of the architecturally singular platforms than the original theorem. In contrast to the known Stewart-Gough platforms which have only six constraints in distances between points, the theorem permits determining the Stewart-Gough platforms with six distance or/and angular constraints between six pairs of points, lines, and/or planes in the base and platform, respectively. These results are of interest for control, on-line simulation and performance analysis of the Stewart-Gough platforms, especially due to their chaotic behavior that lead to their destruction.

The transition between the chaos and hyperchaos is a feature of such platforms, in whose behavior it was observed an infinite number of unstable periodic orbits which becomes unstable in the least two directions in the vicinity of a transition point. These orbits undergo the instability with respect to all directions, exhibiting the riddling bifurcation which explains the appearance of the hyperchaoticity. The great number of tongues anchored at these orbits and the riddling bifurcation have the effect of the growing of the attractor, i.e. the orbits stretch in all directions and the chaotic attractor grows becoming a hyperchaotic attractor. As expected, the chaotic behavior leads finally to the destruction of the platform by the detachment of the legs.

Acknowledgements. This work was supported by a grant of the Romanian ministry of Research and Innovation, CCCDI-UEFISCDI, project number PN-III-P1-1.2-PCCDI-2017-0221/59PCCDI/2018 (IMPROVE), within PNCDI III.

REFERENCES

1. DUPORCQ, E., *Sur la correspondance quadratique et rationnelle de deux figures planes et sur un déplacement remarquable*, C.R.Seances Acad.Sci., 126, 05-1406, 1898.
2. HUSTY, M., *Borel's and R. Bricard's papers on displacements with spherical paths and their relevance to self-motions of parallel manipulators*, in: M. Ceccarelli (Ed.), International Symposium on History of Machines and Mechanisms, Kluwer, 163–172, 2000.
3. BOREL, E., *Mémoire sur les déplacements à trajectoires sphériques*, Mém. Présent. Var. Sci. Acad. Sci. Natl. Inst. Fr., 33(1), 1–128, 1908.
4. BRICARD, R., *Mémoire sur les déplacements à trajectoires sphériques*, J. École Polytech., 11 (2), 1–96, 1906, 1906.
5. KARGER, A., *Parallel manipulators and Borel–Bricard's problem*, Comput. Aided Geom. Des. 27(8), 669–680, 2010.
6. NAWRATIL, G., *Review and recent results on Stewart Gough platforms with self-motions*, Appl. Mech. Mater., 162, 151–160, 2012.
7. DUPORCQ, E., *Premiers principes de géométrie moderne*, Guthier-Villars, 1899.
8. Pottmann, H., Wallner, J., *Computational Line Geometry*, Springer, 2001.
9. STEWART, D., *A platform with 6 degrees of freedom*, Proc. Inst. Mech. Eng., vol. 180, 371–386, 1966.
10. LEWIS, D., RATIU, T., SIMO, J.C., MARSDEN, J.E., *The heavy top: a geometric treatment*, Nonlinearity, 5(1), 1992.
11. DASGUPTA, B., MRUTHYUNJAYA, T.S., *The Stewart platform manipulator: A review*, Mechanism and Machine Theory, 35(1), 15–40, 2000.
12. SHAW, D., *Cutting path generation of the Stewart-platform-based milling machine using an end-mill*, Int. J. Prod. Res., 39(7), 1367, 2001.
13. BENETTIN, G., FASSÒ, F., GUZZO, M., *Fast rotations of the rigid body: a study by Hamiltonian perturbation theory*, Part II: Gyroscopic rotations, Nonlinearity, 10(6), 1997.
14. NAWRATIL, G., *Correcting Duporcq's theorem*, Mechanism and Machine Theory, 73 282-295, 2014.
15. BRADEN, H.W., ENOLSKI, V.Z., FEDOROV, YU N., *Dynamics on strata of trigonal Jacobians and some integrable problems of rigid body motion*, Nonlinearity, 26(7), 2013.
16. LAZARD, D., *Generalized Stewart platform: How to compute with rigid motions?* in Proc. IMACS ACA, Lille, France, Jun., 85–88, 1993.
17. MOURRAIN, B., *The 40 generic positions of a parallel robot*, in Proc. ISSAC, M. Bronstein, Ed. 173–182, 1993.
18. WANG, R., ZHANG, X., *Optimal design of a planar parallel 3DOF nanopositioner with multi-objective*, Mechanism and Machine Theory, vol.112, 61-83, 2017.
19. RAGHAVAN, M., *The Stewart platform of general geometry has 40 configurations*, ASME J. Mech. Design, vol. 115, 277–282, 1993.

20. RONGA, F., VUST, T., *Stewart platforms without computer ?* in Proc. Int. Conf. Real Analytic and Algebraic Geom., New York: Walter de Gruyter, 196–212, 1995.
21. DIETMAIER, P., *The Stewart–Gough platform of general geometry can have 40 real postures*, in Advances in Robot Kinematics: Analysis and Control, J. Lenarcic and M. L. Hust, Eds. Norwell, MA: Kluwer, 7–16, 1998.
22. MERLET, J.P., *Parallel Robots*, New York: Springer-Verlag, 2000.
23. MERLET, J.P., *Singular configurations of parallel manipulators and Grassmann geometry*, Int. J. Robot. Res. 8(5) (1992) 45–56.
24. WRÓBLEWSKA-KAMIŃSKA, A., *Existence result for the motion of several rigid bodies in an incompressible non-Newtonian fluid with growth conditions in Orlicz spaces*, Nonlinearity, 27(4), 2014.
25. HAUNSTEIN, J.D., SHERMAN, S.N., WAMPLER, C.W., *Exceptional Stewart-Gough platforms, Segre embeddings, and the special Euclidean group*, University of Notre dame, Hesburgh Libraries Curate ND, 2017.
26. ROBERTS, R.M., DE SOUSA DIAS, M.E.R., *Bifurcations from relative equilibria of Hamiltonian systems*, Nonlinearity, 10(6), 1997.
27. FEIREISL, E., HILLAIRET, M., Š. NEČASOVÁ, Š., *On the motion of several rigid bodies in an incompressible non-Newtonian fluid*, Nonlinearity, 21(6), 2008.
28. KAPITANIAK, T., *Chaos synchronization and hyperchaos*, Journal of Physics: Conference Series, 23, 317-324 International Conference on Control and Synchronization of Dynamical Systems, 2005.
29. ROSSLER, O.E., *An equation for continuous chaos*, Physics Letters, A57, 397, 1976.
30. PEINKE, M.J., PARISI, J., ROSSLER, O.E., STOOP, R., *Encounter with chaos*, Springer, Berlin, 1992.
31. KAPITANIAK, T., CHUA, L.O., ZHONG, G.Q., *Experiment hyperchaos in coupled Chua's circuits*, IEEE Transactions on Circuits and Systems, I, 41, 499-503, 1994.
32. KAPITANIAK, T., STEEB, W.H., *Transition to hyperchaos in coupled generalized van der Pol equations*, Physics Letters, A152, 33, 1991.
33. KAPITANIAK, T., MAISTRENKO, Y., GREBOGI, C., *Bubbling and riddling of higher-dimensional attractors*, Chaos, Solitons and Fractals, 17, 61-66, 2003.
34. MUNTEANU, L., BRIȘAN, C., CHIROIU, V., DUMITRIU, D., IOAN, R., *Chaos-hyperchaos transition in a class of models governed by Sommerfeld effect*, Nonlinear Dynamics, 78(3) 1877-1889, 2014.
35. MUNTEANU, L., CHIROIU, V., SIRETEANU, T., *On the response of small buildings to vibrations*, Nonlinear Dynamics, 73(3), 1527-1543, 2013.
36. BLAISTEN-BAROJAS, Y.LI, E., *Nonlinear coupling between rotation and internal vibration in simple molecular system*, Journal of Physics B: Atomic, Molecular and Optical Physics, 30, 309-318, 1997.

Received September 10, 2018